

(NASA-CF-137229) A METHOD FOR  
DETERMINING THE PREFERRED ORIENTATION OF  
CRYSTALLITES NORMAL TO A SURFACE (Alfred  
Univ.) 19 p HC \$4.00 CSCI 20B

N74-19369

Unclas  
G3/26 32738

# A METHOD FOR DETERMINING THE PREFERRED ORIENTATION OF CRYSTALLITES NORMAL TO A SURFACE

Robert L. Snyder and William L. Carr

New York State College of Ceramics  
Alfred University  
Alfred, New York

Many polycrystalline materials exhibit anisotropy in their thermal, electrical, optical and mechanical properties owing to preferred orientations in crystallite packing. A knowledge of the directions and degree of preferred orientation is essential in understanding and predicting the physical properties of these materials. The directions of preferred orientation in a specimen are a function of crystallite shape and the process used to form the body. In extruded or rolled materials it is common to find two types of orientation, one normal to the surface of the body, the second within the surface in the rolling or extrusion direction<sup>1,2</sup>. Fabrication techniques based on casting, deposition or pressing, however, will introduce preferred orientations normal to the surface only, with crystallite directions within the surface at random.

The most common method of representing preferred orientation is to construct a stereographic projection of the normals to a crystallographic plane, called a pole figure<sup>3,4</sup>. Other techniques such as representing the angular distribution of a particular direction in a crystallographic reference frame (inverse pole figure)<sup>5-8</sup> or analytical methods<sup>9,10</sup> have been developed. The data required by these techniques for displaying preferred orientation is obtained by measuring the orientation of a large number of crystallites. This may be

done visually using etch-pit or Laue techniques which, experimentally, are both tedious and difficult<sup>11</sup>. Most workers take advantage of the fact that the intensities of X-ray diffraction maxima are proportional to the number of crystallites whose crystallographic plane normals bisect the incident and diffracted beams. To measure the data necessary to obtain a pole figure for a particular crystallographic direction  $h k \ell$ , the incident and diffracted X-ray beams are set so that each make an angle  $2\theta_{hkl}$  with respect to the specimen. Intensity data are then recorded at various specimen angles with respect to the diffractometer geometry, holding  $2\theta$  constant<sup>12,13</sup>. Such pole figure devices, though complex and expensive, are in common use and often automated<sup>14,15</sup>.

In principle all of the preferred-orientation information for the direction normal to a surface will be contained in the intensity differences between X-ray diffraction peaks for a sample with a preferred orientation and one with a fully random crystallite orientation. If the sample was formed in a way that produces only orientations normal to the surface, an X-ray powder diffractometer tracing will contain the needed information. If there are also preferred orientations within the surface, then the sample should be rotated about an axis that bisects the incident and diffracted beams, scanning  $2\theta$ , after each incremental rotation. The many experimental difficulties in obtaining the diffraction pattern of a fully random sample may be avoided by calculating the powder diffraction pattern from crystal structure parameters. The calculated diffraction peak intensities will correspond to the intensities of an experimental pattern having a completely random crystallite orientation. Thus a full analysis of crystallite orientation should be available from a comparison of an observed diffraction pattern with a calculated "ideal" pattern.

## EXPERIMENTAL

X-ray diffraction patterns were obtained with Cu K $\alpha$  radiation using an X-ray diffractometer, equipped with a

graphite monochromator. The alumina sample used in this study was obtained from Dr. P.H. Crayton; it had been prepared by hot-pressing a mixture of 99.0%  $\text{Al}_2\text{O}_3$  and 1%  $\text{MgO}$ . The diffraction pattern was obtained so that the pressing direction, normal to the wafer-shaped specimen, bisected the incident and diffracted X-ray beams. All but four low-intensity peaks in the observed pattern corresponded to reported peaks in  $\alpha\text{-Al}_2\text{O}_3$  (corundum). The four non-alumina peaks were identified as the four strongest peaks in  $\text{MgAl}_2\text{O}_4$  spinel<sup>16</sup> and were deleted from the pattern.

The barium hexaferrite sample used was supplied by Dr. J.S. Reed. It was prepared by pressure filtration with a magnetic field in the direction of filtration. The diffraction pattern of the wafer-shaped sample was obtained in the same manner as for alumina. A number of peaks were observed which did not correspond to the calculated pattern; these were attributed to stoichiometries differing from  $\text{BaO} \cdot 6\text{Fe}_2\text{O}_3$ . These peaks were not removed from the observed pattern but left to test the abilities of our computer program to reject them. The third material studied was aragonite ( $\text{CaCO}_3$ ). The diffraction pattern was chosen somewhat randomly from among the orthorhombic materials for which the National Bureau of Standards have published X-ray diffraction patterns<sup>17</sup>. An orthorhombic material was desired to test the procedure on a low-symmetry material. NBS data were used because of its high quality and the high probability of there being as little orientation as possible in it, thus giving a random orientation to test our procedure.

The calculated diffraction patterns were obtained using a local modification of a program first developed by D.K. Smith<sup>18</sup>. The parameters used in calculating the powder patterns are given in Table I. All patterns were calculated for copper radiation using a Cauchy peak profile. Anomalous dispersion corrections for barium and iron were included in the calculation of structure factors for barium hexaferrite. The widths of the peaks at half-height were calculated in all cases to be  $0.07^\circ$  at  $40.0^\circ 2\theta$ .

Table I. Parameters Used in Calculating Powder Patterns.

Compound	Atom	Multi- plicity	X	Y	Z	B or $\beta_{11}$
BaO · 6Fe <sub>2</sub> O <sub>3</sub> <sup>19-20</sup> a=b=5.889 Å c=23.182 Å $\alpha=\beta=90^\circ$ $\gamma=120^\circ$ P <sub>6<sub>3</sub>/m mc</sub>	Ba <sup>+2</sup> (d)	.125	.3333	.6667	.7500	1.0
	Fe <sup>+3</sup> (a)	.125	0.0	0.0	0.0	1.0
	Fe <sup>+3</sup> (b)	.125	0.0	0.0	.250	1.0
	Fe <sup>+3</sup> (f)	.250	.3333	.6667	.028	1.0
	Fe <sup>+3</sup> (f')	.250	.3333	.6667	.189	1.0
	Fe <sup>+3</sup> (k)	1.0	.167	.334	.108	1.0
	O <sup>-2</sup> (e)	.25	0.0	0.0	.150	1.0
	O <sup>-2</sup> (f)	.25	0.0	0.0	-.050	1.0
	O <sup>-2</sup> (h)	.50	.3333	.6667	.250	1.0
	O <sup>-2</sup> (k)	1.0	.167	.334	.050	1.0
	O <sup>-2</sup> (k')	1.0	.50	1.0	.150	1.0
Al <sub>2</sub> O <sub>3</sub> <sup>21</sup> a=b=4.7589 Å c=12.9910 Å $\alpha=\beta=90^\circ$ $\gamma=120^\circ$ R <sub>3c</sub>	Al <sup>+3</sup>	.6667	0.0	0.0	.352	1.0
	O <sup>-2</sup>	1.0	.306	0.0	.250	1.0
CaCO <sub>3</sub> <sup>22</sup> a=7.9792 Å b=5.7499 Å c=4.9677 Å $\alpha=\beta=90^\circ$ P <sub>bnm</sub>	Ca <sup>+2</sup>	.5	.4151	.7597	.250	.0024
	C <sup>+4</sup>	.5	.7623	-.0855	.250	.0029
	O <sup>-2</sup>	.5	.9234	-.0953	.250	.0025
	O <sup>-2</sup> '	1.0	.6804	-.0871	.4741	.0043
		$\beta_{22}$	$\beta_{33}$	$\beta_{12}$	$\beta_{13}$	$\beta_{23}$
	Ca <sup>+2</sup>	.0048	.0063	.0001	.0000	.0000
	C <sup>+4</sup>	.0039	.0060	.0002	.0000	.0000
	O <sup>-2</sup>	.0080	.0131	.0003	.0000	.0000
	O <sup>-2</sup> '	.0078	.0061	.0005	.0012	.0002

The barium hexaferrite and alumina samples were observed with an Etec SEM. The barium hexaferrite shown in Fig. 1 is predominately in the form of hexagonal-shaped platelets with 001 normal to the six-fold symmetry axis. Though crystallites of all orientations were observed, there was a definite

Fig. 1.  $\text{BaO} \cdot 6\text{Fe}_2\text{O}_3$   
specimen; SEM 30,000X.

Fig. 2.  $\text{Al}_2\text{O}_3$  specimen;  
SEM 20,000X.

predominance of crystallites lying with 001 normal to the direction of filtration. The alumina specimen shown in Fig. 2 has been sintered to the point of loss of identity of most crystallites, but the specimen does appear to have a layer-like structure in the direction normal to hot-pressing. Normally, alumina shows a tendency to orient with 001 normal to the surface<sup>1</sup>.

## PROCEDURE

The problem which immediately arises, when one tries to compare observed X-ray intensities with those calculated, is that they are not on the same scale. When the observed pattern is from a randomly oriented sample, the conventional  $I/I_{\text{max}}$  values will equal those of the calculated pattern within statistical error. But when a preferred orientation occurs, the intensity of the highest peak ( $I_{\text{max}}$ ) will change relative to all other observed intensities, thus putting the  $I/I_{\text{max}}$  values on a new scale. In order to scale the observed-to-calculated values we would need a law of conservation of relative intensity (i. e., the sum of the fractional decreases in peak intensities equals the sum of fractional increases). Due to the fact that crystallites can orient into or away from directions whose reflections have zero intensity, such a law is impossible and we are left with having to seek a method of comparison not involving scaling.



One approach can be based on the fact that, as the fraction of crystallites oriented in a particular direction increases, not only will the reflection intensities in that zone increase, but also the intensities of those reflections whose plane normals make a small angle with the zone. This will result from the increased probability of finding crystallites almost, but not quite, perfectly oriented. Thus the slope of a plot of  $(I_{\text{obs.}} - I_{\text{calc.}})_{\text{hkl}}$  vs.  $\Phi$ , ( $\Phi$  is the angle the normal to each plane  $(\text{hkl})$  makes with a particular zone) should be negative at low angles for a zone of preferred orientation, first scaling the  $\Delta I$  values to make those at the zone ( $\Phi = 0.0$ ) zero. Similarly, the slope should be positive for a zone of anti-preferred orientation, i.e., an orientation which shows a decrease in the number of crystallites displaying it.

Fig. 3 shows a plot of this type for the 100 zone of barium hexaferrite and illustrates the weaknesses of this method. Statistical errors in the observed intensities and differing rates of change in  $I_{\text{O}} - I_{\text{C}}$ , depending on the direction from which the zone is approached, obscure any trend. The principal weakness is the dependence on the occurrence of reflections making a small angle with the zone. Thus the criteria for a procedure to analyse preferred orientation

Fig. 3.  $(I_{\text{obs.}} - I_{\text{calc.}})_{\text{hkl}}$  vs.  $\Phi$  (the angle that the  $\text{hkl}$  plane normal makes with the zone) for the 100 zone of barium hexaferrite. Scaled so that  $\Delta I$  is zero at  $\Phi = 0.0$ .

001 ZONE

IO - IC

-85.17 -85.17 -85.17 -85.17 -85.17 -85.17 -85.17 -85.17 -85.17 -85.17 -85.17 -85.17 -85.17 -85.17 -85.17 -85.17 -85.17 -85.17 -85.17 -85.17

00 9.00 18.00 27.00 36.00 45.00 54.00 63.00 72.00 81.00 90.00  
ANGLE FROM ZONE

BA0.6FE203



should be: 1.) It must be independent of scale factor, 2.) The function evaluated at each point in space must depend on a large number of intensities to minimize the large relative error in weak reflections, and 3.) The function must not be restricted to evaluation at only those points for which there are observed reflections.

In reference to the 001 orientation in barium hexaferrite, Lotgering<sup>23</sup> has defined an orientation factor as  $f = (p_o - p_r) / (1 - p_r)$  where  $p_o = \sum_l I_{00l} / \sum_{hkl} I_{hkl}$  for an oriented sample.  $p_r$  is the same function referred to a randomly oriented sample. When a random sample can be prepared experimentally and care is taken to keep the diffraction pattern for it, and for the oriented sample, on the same scale,  $f$  will be zero for a completely random orientation and unity, for a complete 001 orientation. Gillam and Smethurst<sup>24</sup>, in trying to relate an orientation factor to the total magnetic moment of a sample, modified Lotgering's  $p$  factor to include the magnetic components of crystallites not completely aligned. Their "magnetic quality factor" is  $q = \sum I_{hkl} \cos \Phi_{hkl} / \sum I_{hkl}$  where  $\Phi_{hkl}$  is the angle between the 001 and  $hkl$  planes. A formula of this type can be generalized to meet the criteria outlined above.

We define a quantity  $Q_{hkl}$  for any direction  $hkl$  in reciprocal space as

$$Q_{hkl} = \frac{\sum_{h'k'l'} I_{h'k'l'} \cos \varphi_{hkl}}{\sum_{h'k'l'} I_{h'k'l'}} \quad (1)$$

where  $h'k'l'$  refer to those reflections for which we have observed or calculated intensity data and  $\varphi_{hkl}$  is the angle between the normals to planes  $hkl$  and  $h'k'l'$ . A value for  $Q$  can be evaluated for any arbitrary direction  $hkl$  whether or not we have a reflection corresponding to that direction. Each  $Q$  value is a function of the intensities of all reflections, minimizing the effect of an error in any one intensity value and the problem of a high relative error in weak reflections.  $Q_{hkl}$  may be thought of as the net fractional vector compon-

ent of total intensity in the direction  $hkl$ . Since any scale factor between our observed and calculated intensities must be a constant which multiplies all observed or calculated intensity values, it will factor out of the two summations in Eq. 1 and cancel on division, leaving  $Q_{hkl}$  independent of scale.

The  $Q$  function can be applied to show the directions of preferred, antipreferred and nonpreferred orientation\* in any system for which observed and calculated diffraction patterns can be obtained.  $Q$  values from both the observed and calculated intensities may be evaluated for a large number of directions  $hkl$ . For each direction a  $\Delta Q_{hkl}$  value may be calculated as  $(Q_{\text{observed}})_{hkl} - (Q_{\text{calculated}})_{hkl}$ . Now the angle  $\Phi$  between each  $hkl$  direction and any zone of interest may be calculated and a plot of  $\Delta Q_{hkl}$  vs.  $\Phi$  may be constructed for that zone. A negative slope indicates that the zone is a direction of preferred orientation. A positive slope indicates a direction of antipreferred orientation. A scatter plot with low values for  $\Delta Q$  indicates a zone of nonpreferred orientation.

A computer program named PREF has been written in FORTRAN for carrying out this procedure and is available from the first author. The program reads the observed and calculated reflections, matches them within a preset error window and eliminates any non-matching peaks in the observed pattern.  $Q_{\text{obs.}}$  and  $Q_{\text{cal.}}$  values are then evaluated for all directions  $hkl$  making an angle of  $10^\circ$  or more with each of the seven principal zones, 100, 010, 001, 110, 101, 011 and 111. Plots of  $\Delta Q_{hkl}$  vs.  $\Phi$  are then produced for all seven principal zones on a CALCOMP plotter.

---

\*The term preferred orientation is used to indicate a direction into which crystallites have oriented, antipreferred refers to a direction out of which crystallites have oriented and nonpreferred is used to indicate a direction which shows no orientation effects.

1. TITLE: C x 3 30 x 49 working  
 2. AUTHOR: LGL 27 x 45 final  
 3. SUBJECT: L. P. de Ror

# RESULTS AND DISCUSSION

Figs. 4 and 5 show plots of  $(Q_{obs.})_{hkl}$  and  $(Q_{cal.})_{hkl}$  vs.  $\Phi$  for the 001 zone of barium hexaferrite. The curves show a maximum in the region of  $\Phi = 50^\circ$ . This is due to the fact that a number of very intense reflections occur in

AUTHORS' NAMES

AUTHORS' AFFILIATION

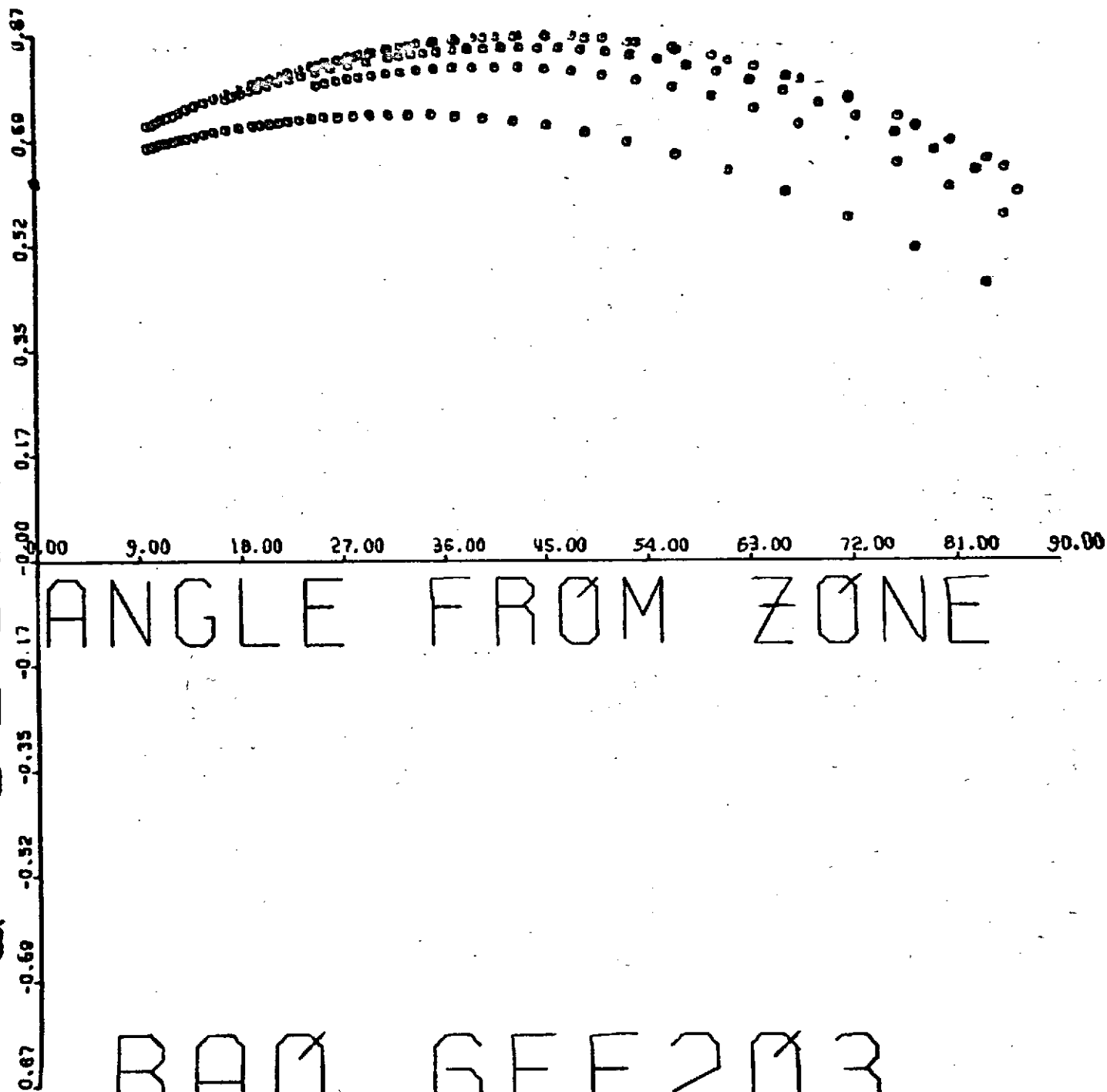
AND ADDRESS

- FIRST LINE OF TEXT (FIRST PAGE)

Fig. 4.  $(Q_{obs.})_{hkl}$  vs.  $\Phi$  for the 001 zone of barium hexaferrite sample.

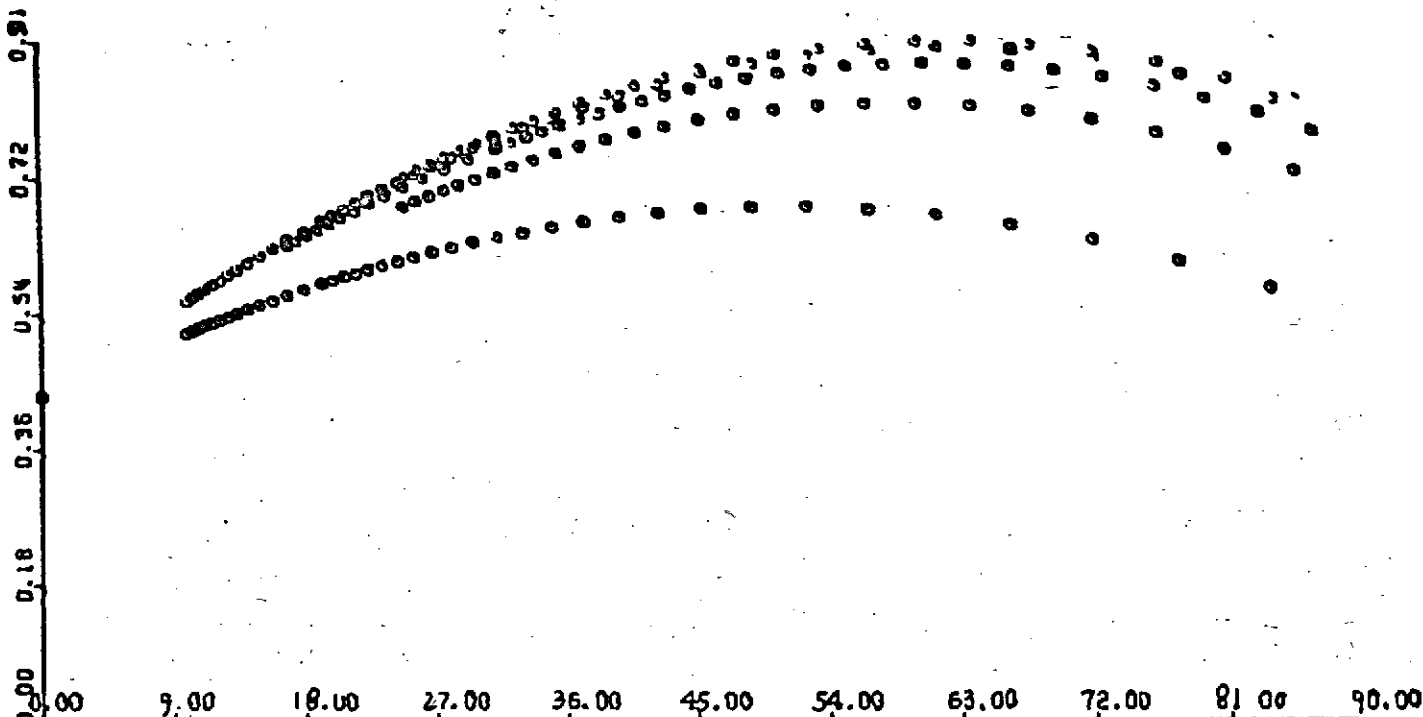
Fig. 5.  $(Q_{cal.})_{hkl}$  vs.  $\Phi$  for the 001 zone of barium hexaferrite sample.

001 ZONE  
OBSERVED



BAO. 6FE203

Q CALCULATED  
001 ZONE



ANGLE FROM ZONE

BA0.6FE203

this range. The general shape of the curves will vary from compound to compound depending on the intensity distribution, which is a function of the crystal structure. The magnitude of  $Q$  for any particular class of reflections will also depend on this intensity distribution and will thus vary with the structure type being looked at. Each point on the lowest curve in Fig. 5 is in the reflection class  $01\ l$ , moving up the plot the next curves are due to  $11\ l$ ,  $02\ l$ , ending with the top curve due to  $10\ l$  directions. Since barium hexaferrite shows no reflections with indices of the type of  $01\ l$  we should expect the  $Q$  curve based on  $01\ l$  directions to have the lowest values. The gap in all the curves between  $0^\circ$  and  $10^\circ\ \Phi$  is simply the result of our program not generating  $Q$  values in this interval. Notice that the only difference between the  $Q_{\text{obs.}}$  and  $Q_{\text{cal.}}$  plots is in the absolute magnitude of the  $Q$  values,  $Q_{\text{obs.}}$  being higher than  $Q_{\text{cal.}}$  at low  $\Phi$  and lower at high  $\Phi$ .

Figs. 6, 7 and 8 show the  $\Delta Q$  vs.  $\Phi$  plots for the seven principal zones of barium hexaferrite, alumina and aragonite, respectively. In each of these plots the  $\Delta Q$  values have been scaled so as to make the  $\Delta Q$  value at  $\Phi = 0.0^\circ$  zero. In the cases of barium hexaferrite and alumina, the negative slope of the  $001$  zone plots indicate, as expected, that  $001$  is a zone of preferred orientation. The positive slopes of each of the other six plots indicate that they are all zones of anti-preferred orientation. In the case of alumina the magnitudes of the  $\Delta Q$  values are much smaller than those for barium hexaferrite; this indicates that the extent of  $001$  orientation in barium hexaferrite is much greater than in the case of alumina.

The NBS aragonite sample, the  $\Delta Q$  plots for which are shown in Fig. 8, shows a different behavior. The  $001$  zone shows a symmetric scatter plot, and is thus a direction of non-preferred orientation. The increase in the number of points as  $\Phi$  increases is an artifact due to the manner in which the data points were generated by the PREF program. The  $010$  and  $011$  zones on the other hand show clear evidence of antipreferred orientation, while the  $100$  and  $101$  zones show preferred orientation. The slight asym-

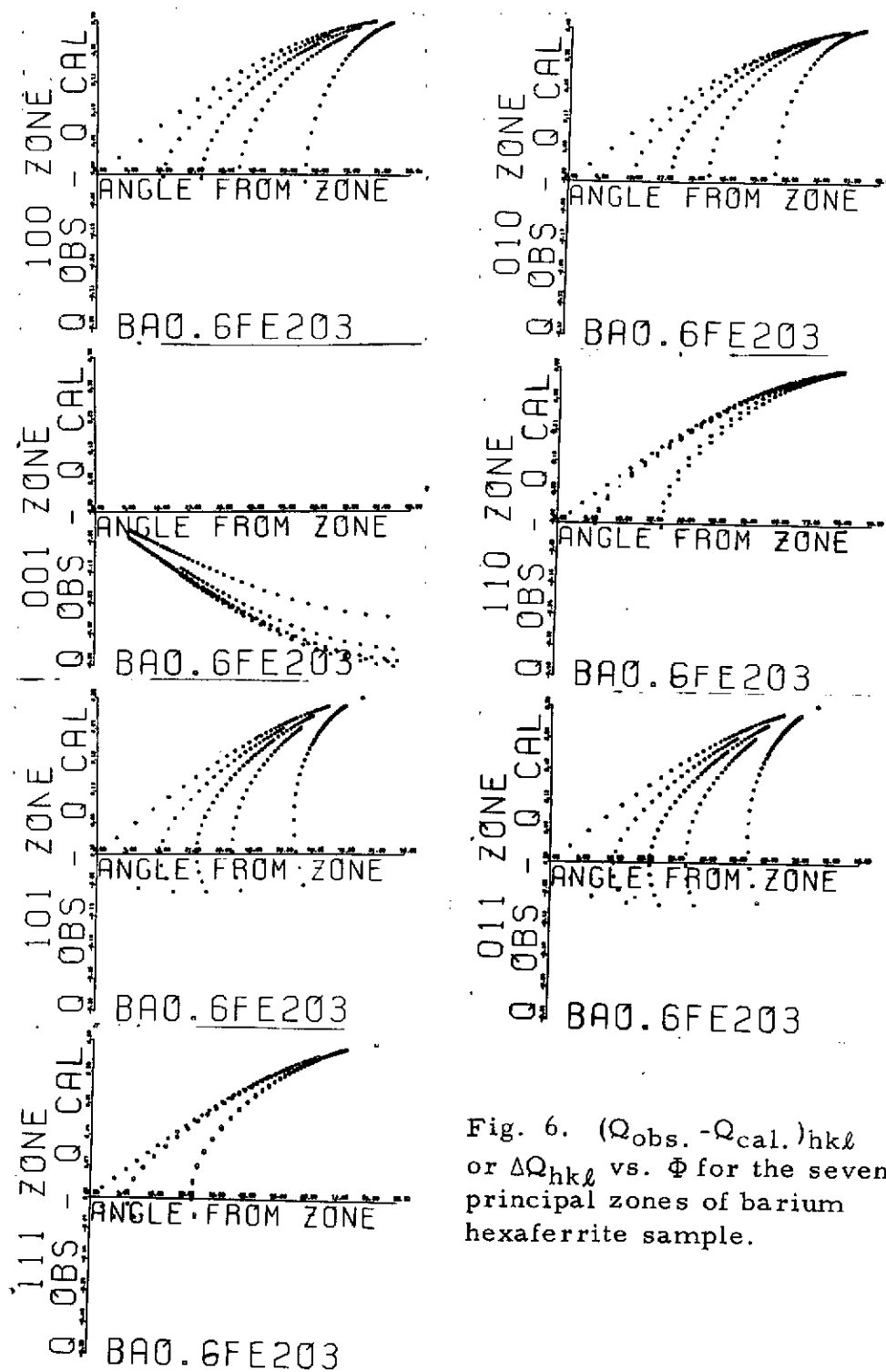


Fig. 6.  $(Q_{\text{obs}} - Q_{\text{cal}})_{hkl}$  or  $\Delta Q_{hkl}$  vs.  $\Phi$  for the seven principal zones of barium hexaferrite sample.

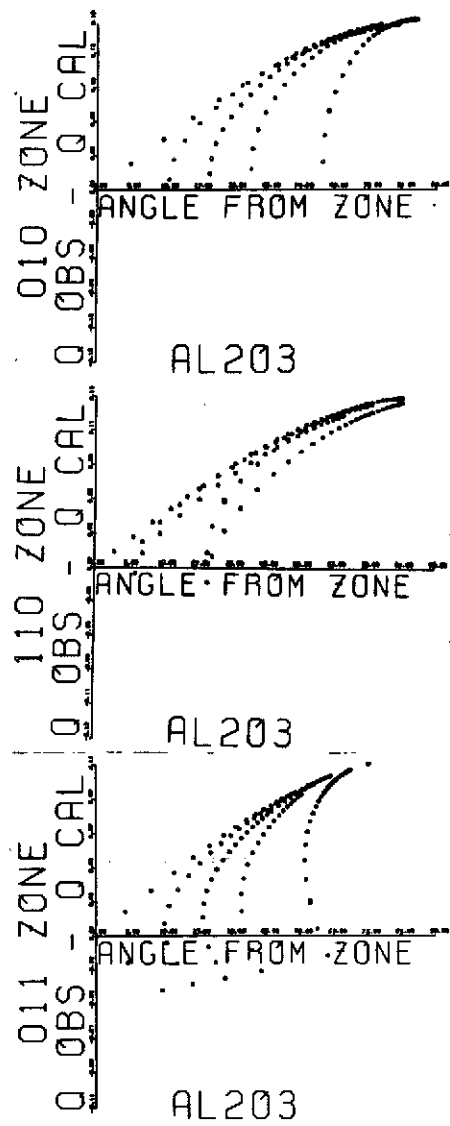
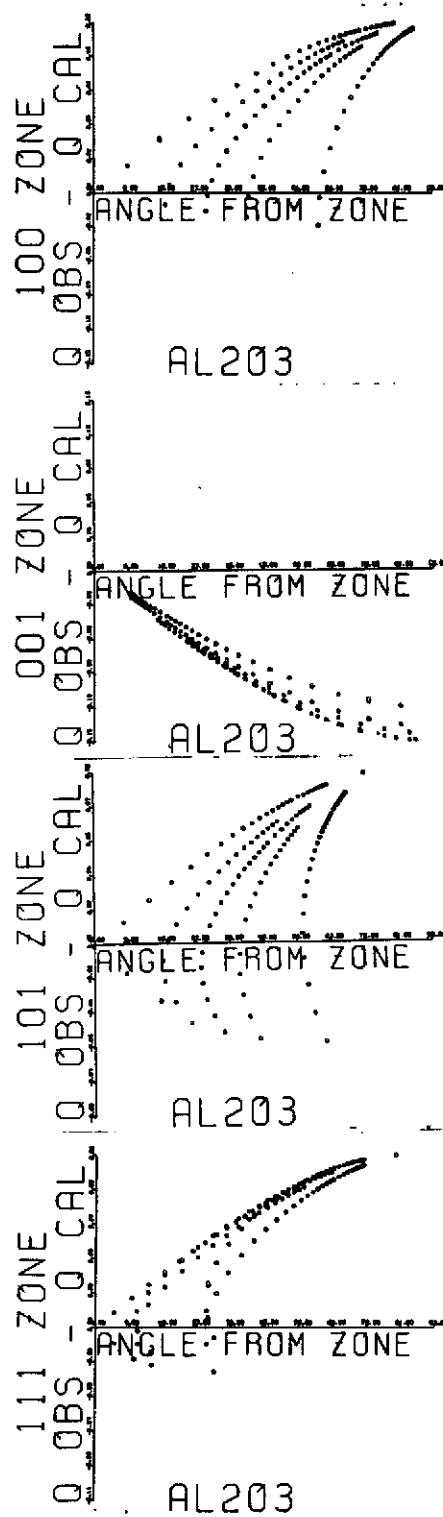


Fig. 7.  $\Delta Q_{hkl}$  for the seven principal zones of alumina sample.



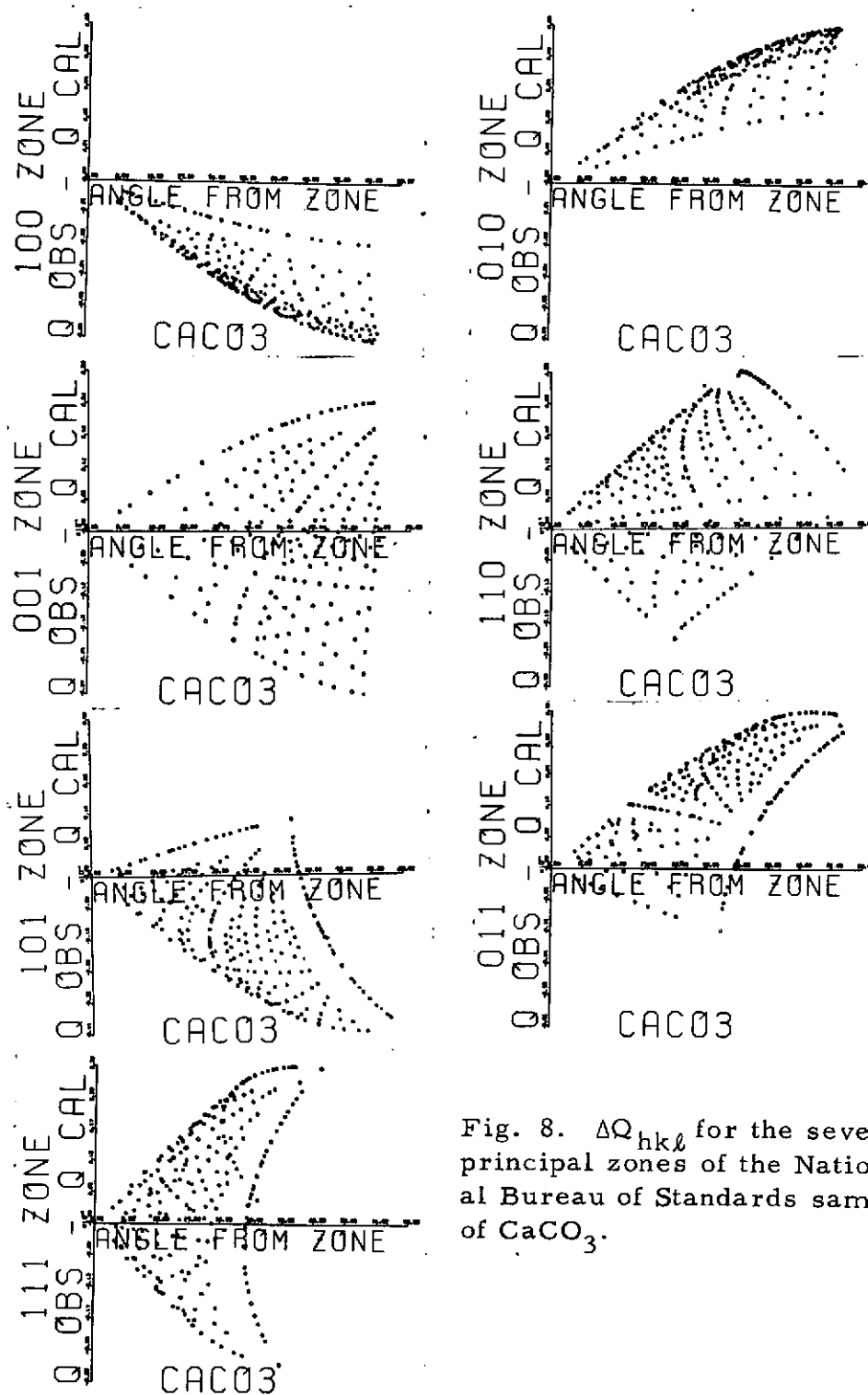


Fig. 8.  $\Delta Q_{hkl}$  for the seven principal zones of the National Bureau of Standards sample of  $\text{CaCO}_3$ .

metry toward a positive slope in the 110 and 111 zones indicates a slight antipreferred orientation. Here the  $\Delta Q$  values are very small, indicating that these orientation effects are slight. The authors have yet to run a material, no matter how carefully the sample is prepared, that did not show some slight degree of orientation.

### CONCLUSION

Differences between the  $Q$  values for observed and calculated diffraction patterns show the directions of preferred crystallite orientation in a material. Additional information on which zones the crystallite orientation avoids is also yielded by the procedure. The magnitude of the  $\Delta Q$  values appear to correlate with the extent of orientation. The quantification of this procedure to yield directional, enhancement of property coefficients is currently under study and will be the subject of a subsequent report.

### ACKNOWLEDGMENTS

The authors would like to express appreciation to colleagues Drs. James Reed and Phillip Crayton for supplying the oriented samples and Mr. Ward Votava for the electron micrographs. This work was supported in part by NASA.

### REFERENCES

1. J. L. Pentecost and C. H. Wright, *Advance in X-Ray Analysis* 4, 174-181 (1963).
2. P. R. Morris and A. J. Heckler, *Advances in X-Ray Analysis* 11, 454-472 (1967).
3. H. P. Klug and L. E. Alexander, *X-Ray Diffraction Procedures*, Wiley, New York 1954, Chapt. 10.
4. J. R. Holland, *Advances in X-Ray Analysis* 4, 86-93 (1963).
5. G. B. Harris, *Phil. Mag.*, 43, 113-125 (1952).
6. R. Roe, *J. Appl. Phys.* 36, 2024-2031 (1965).

7. R. Roe, J. Appl. Phys. 37, 2069-2072 (1966).
8. J.A. Slane and F. Hultgren, Advances in X-Ray Analysis 14, 231-242 (1972).
9. R.H. Bragg and C.M. Packer, J. Appl. Phys. 35, 1322-1328 (1964).
10. M.N. Klenck, Advance in X-Ray Analysis 11, 447-453 (1967).
11. C.G. Dunn, J. Appl. Phys. 30, 850-857 (1959).
12. B.D. Cullity, Elements of X-Ray Diffraction, Addison-Wesley Co., Reading, Mass., 1956, Chapt. 9.
13. L.G. Schulz, J. Appl. Phys. 20, 1030 (1949).
14. S.L. Lopata and E.B. Kula, Trans. Am. Inst. Mining, Met., Petrol. Engrs. 224, 865 (1962).
15. J.R. Holland, N. Engler and W. Powers, Advances in X-Ray Analysis 4, 74 (1961).
16. H. Saalfeld and H. Hagodzinski, Z. Krist 109, 87-109 (1957).
17. H.E. Swanson, R.K. Fuyat and G.M. Vgrinic, NBS Circular No. 539 Vol. III p. 53.
18. C.M. Clark, D.K. Smith and G.G. Johnson, Dept. of Glosciences, Pennsylvania State University, September, 1973.
19. F. Bertaut, A. Deschamps and R. Pauthenet, C.R. Acad. Sci., Paris, 246, 2594-9597 (1958).
20. V. Adelskold, Ark. Kem. Mineral. Geol., 12(A), 9 (1938).
21. R.E. Newnham and Y.M. DeHaan, Z. Krist, 117, 235-237 (1962).
22. W.L. Bragg, Proc. Roy. Soc. London, 105, 16 (1924).
23. F.K. Lotgering, J. Inorg. Nucl. Chem. 9, 113-123 (1959).
24. E. Gillam and E. Smethurst, Proc. Br. Ceram. Soc. 3, 129-137 (1964).